Nanoscale Res Lett
DOI 10.1007/s11671-009-9400-0

NANO EXPRESS

New Colloidal Lithographic Nanopatterns Fabricated by Combining Pre-Heating and Reactive Ion Etching

Chunxiao Cong · William Chandra Junus · Zexiang Shen · Ting Yu

Received: 26 May 2009 / Accepted: 17 July 2009
© to the authors 2009

Abstract We report a low-cost and simple method for fabrication of nonspherical colloidal lithographic nanopatterns with a long-range order by preheating and oxygen reactive ion etching of monolayer and double-layer polystyrene spheres. This strategy allows excellent control of size and morphology of the colloidal particles and expands the applications of the colloidal patterns as templates for preparing ordered functional nanostructure arrays. For the first time, various unique nanostructures with long-range order, including network structures with tunable neck length and width, hexagonal-shaped, and rectangular-shaped arrays as well as size tunable nanohole arrays, were fabricated by this route. Promising potentials of such unique periodic nanostructures in various fields, such as photonic crystals, catalysts, templates for deposition, and masks for etching, are naturally expected.

Keywords Nanosphere lithography · Nanopatterns · Reactive ion etching · Preheating · Nonspherical · Nonclose-packed

Introduction

Assembling colloidal micro/nano particles into 2-dimensional (2D) or 3-dimensional (3D) ordered arrangements has been of considerable importance in potential applications to biochips and biosensors [1–3], chemical sensors, optical and electronic devices [4], photonic crystals and suface wettability [5, 6], and as templates for designed nanostructures for magnetic data storage memory bits, and surface-enhanced Raman scattering substrates, etc. [7, 8]. A variety of nanofabrication technologies have been developed to prepare large-area 2D or 3D colloidal patterned surfaces, such as self-assembly, spincoating, electric-field-induced electrokinetic flowing, and Langmuir-Blodgett deposition [9–14]. In particular, self-assembly technique, which forming ordered periodic arrays of packed spherical configuration with uniformly sized microspheres, has been applied widely because of its unique features: it is inexpensive, inherently parallel, and enables high-throughput nanofabrication. The template formed by the self-assembly of monodisperse nanospheres on flat surfaces can be used as an etching/deposition mask to fabricate a periodic array of nanosized particles with a technique known as nanosphere lithography (NSL). However, self-assembly alone is greatly restricted to the formation of close-packed spherical pattern. Therefore, one disadvantage of NSL is its limited pattern design. Only triangular-shaped metal nanoparticles can be directly obtained from deposition through monolayer and double layer of close-packed nanospheres.

To extend the limited patterns of NSL, one method is shadow NSL, which is a combination of monolayer-preparation of PS spheres with tilted shadow evaporation [15, 16], the other one is to change the colloidal patterns. In recent years, reactive ion (plasma) etching (RIE) has been widely used to extend the close-packed spherical colloidal patterns based on self-assembly into nonclose-packed nonspherical patterns. It becomes more challenging to fabricate nonspherical particles with controllable shapes, nonclose-packed patterns, and good periodicity in a large scale. Choi et al. [17] employed RIE technique with pure O_2 gas or mixture of CF_4 and O_2 to create 2D and 3D

C. Cong · W. C. Junus · Z. Shen · T. Yu (✉)
Division of Physics and Applied Physics, School of Physical and Mathematical Sciences, Nanyang Technological University, Singapore 637371, Singapore
e-mail: yuting@ntu.edu.sg

Published online: 28 July 2009

nonspherical polystyrene (PS) particle arrays of various shapes by using PS spheres stacking layer by layer, with the top layer acting as mask. One disadvantage of this process is that the area of the arrays with a certain configuration is small because there is no controllable method to fabricate large-area of certain layers of PS spheres until now. Tan et al. [18] and Yan et al. [19] prepared nonclose-packed polystyrene spheres by using a gas mixture of CF_4 and low O_2 content and pure argon plasma etching process, respectively. Only elliptical particles were obtained. Wu et al. [20] fabricated nano-net structure with necks formed between neighboring PS particles by oxygen plasma etching of a monolayer of PS spheres. However, the necks disappeared when the etching time was longer than 3 min, which leading to the uncontrollability of further manipulating the dimension of this novel nano-net structure.

In this work, we demonstrate a simple and inexpensive method to fabricate controllable nonclose-packed nonspherical PS particle arrays with long-range order. The method is based on a combination of colloidal self-assembly, preheating, and oxygen reactive ion etching techniques. The long-range ordered network pattern of PS particle arrays with tunable neck width and length were obtained. The hexagonal- and the rectangular-shaped PS particles were fabricated. Moreover, the round nanoholes were also achieved after oxygen RIE of double layer of PS spheres with preheating. These structures and patterns differ noticeably from the known elliptical-shaped PS particles and triangular nanoholes produced without preheating. Such unique colloidals and their ordered arrays resulted from the strategy demonstrated in this work may have important applications in fields of chemical sensors, photonic crystals, catalysts, biosensors, and can serve as good deposition or etching masks for growth of other 2-dimensional nanostructures, which have shape- and size-dependent properties. The effect of preheating on the fabrication of long-range ordered nonclose-packed nonspherical colloidal nanopatterns was also discussed in this work.

Experimental Procedures

Monodispersed PS spheres (1,000 and 465 nm in diameter) suspensions (2.6 wt% in water, surfactant-free) were purchased from Polysciences, Inc and diluted by mixing with an equal amount of ethanol. The Si substrates were cleaned in an ultrasonic bath with acetone, ethanol, and deionized water at room temperature, and then rinsed using deionized water. A monolayer of highly ordered PS spheres were first self-assembled on water surface using a technique reported by Rybczynski et al. [9] as below. About 5 μL of prepared solutions was dropped onto the surface of a 3 × 3 cm large clean silicon wafer, which was kept in 10% dodecylsodiumsulfate solution for 12 h previously. The wafer was then slowly immersed in the Ø 10 cm glass vessel filled with deionized water and PS spheres started to form a monolayer on the water surface. Such monolayer was then lifted off from the water surface using another cleaned Si substrate, and dried in air at room temperature. Double-layered PS spheres were produced by immersing dry, once-covered substrates into water and lifted off a second layer. Then, the as-prepared monolayer of PS spheres with diameters of 465 and 1,000 nm were put into an airtight oven and preheated for 1 and 2 min, respectively. The airtight oven was heated up to 110 °C before putting samples into it, which is slightly higher than the glass transition temperature of PS (i.e., $T_g = 100$ °C, provided by the PS microsphere manufacturer). Finally, the RIE process was performed by using March PX-250 plasma etching system with power of 70 W and base pressure of 70 mTorr. Pure oxygen gas with flow rate of 100 sccm was used as plasma source to morph the preheated close-packed PS spheres monolayer into arrays of various nonclose-packed nonspherical PS particle patterns with varying RIE durations. The morphologies of the samples were characterized by field emission scanning electron microscopy (FE-SEM, JEOL JSM-6700F).

Results and Discussion

Figure 1b2–b4 shows the SEM micrographs of network PS particle arrays with tunable neck width and length which were produced after oxygen RIE of monolayer of PS spheres with preheating. To reveal the effect of preheating, the morphologies of PS particle arrays produced after oxygen RIE of monolayer of PS spheres without preheating were also shown in Fig. 1a2–a4. Here, the initial size of PS sphere is 465 nm, and the preheating time is 1 min because the longer duration of heating could melt the PS spheres and merge them into a film. The PS spheres cannot be separated from each other even after oxygen RIE. It can be seen that the network pattern, which was composed of each PS particle with six necks connecting to the nearest-neighbor PS particles, was obtained by combining preheating and oxygen RIE. The network pattern kept long-range order even the etching time was as long as 700 s (Fig. 1b4). However, for the PS particles without preheating, though there was also a neck formation between neighboring PS particles when the etching duration was $<$300 s, most of the necks disappeared when the etching time was beyond this value (Fig. 1a3). The PS particle arrays became disordered when the etching time was longer than 450 s (Fig. 1a4). The loss of periodicity is mainly due to the plasma bombardment which may knock away the isolated tiny spheres [21]. The neck length and

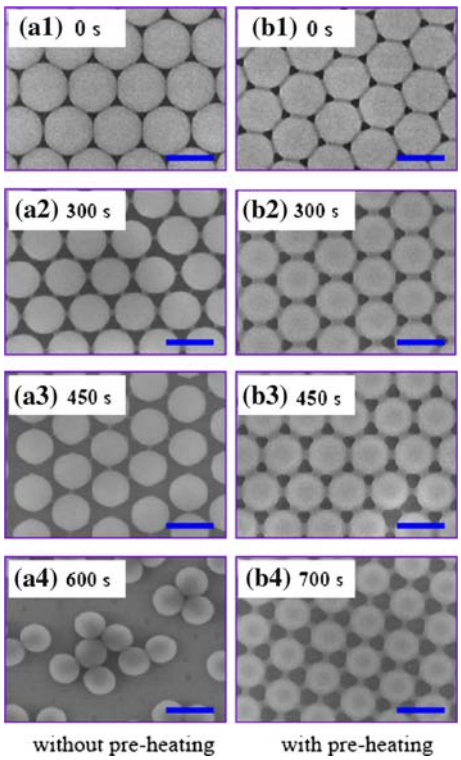

Fig. 1 SEM images of the PS particle monolayer (465 nm in diameter) after oxygen RIE for different time: **a1**–**a4** 0, 300, 450, 600 s, without preheating; and **b1**–**b4** 0, 300, 450, 700 s, with preheating, respectively. The *scale bar* is 500 nm in each image

width as a function of RIE time are plotted in Fig. 2 for the preheated series, showing that the length (or width) of the necks increases (or decreases) linearly with the increasing oxygen RIE time. The neck length and width can be easily tuned from about 30 to 80 nm and 150 to 80 nm, respectively, by increasing the oxygen RIE time. It can be seen from Fig. 1a1, b1 that the preheating leads to the contact between neighboring PS particles changing from point contact to face contact, and preheating also makes the PS particles stick tightly on the substrate. Correspondingly, the PS particles with preheating connect each other tighter than those without preheating, thus they can keep long-range order even when the etching time was as long as 700 s. The controllable necks between adjacent PS particles are formed by anisotropic RIE of the joint of the face contact. Therefore, the formation of long-range ordered network pattern with tunable neck width and length can be attributed to anisotropic RIE and preheating, which converts the point contact between original spheres (see Fig. 1a1) into extended face contact between regular polygons (see Fig. 1b1), as well as makes the PS spheres stick tightly to the substrate. Therefore, preheating plays a very important role not only in fabricating this new controllable network pattern but also in keeping long-range order.

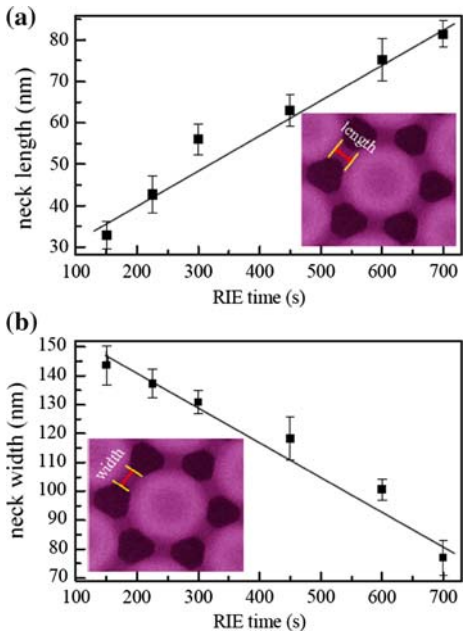

Fig. 2 Plot of **a** neck length, and **b** neck width of the necks formed in the preheated monolayer of PS spheres (465 nm in diameter) as a function of oxygen RIE time

Figure 3 shows the rectangular-shaped PS particle arrays fabricated by oxygen RIE of inhomogeneous densified monolayer of PS spheres with 465 nm in diameter. Rodlike shape of the apertures are formed in the inhomogeneous densified colloidal monolayer after preheating for 1 min (Fig. 3a), which differs noticeably from the triangular apertures formed in the standard PS spheres monolayer. The formation mechanism of the rodlike shaped apertures has been discussed in Ref. [22] in detail. The PS particles in the inhomogeneous densified arrays have been deformed to quasi-rectangular shape from spherical shape by preheating. Consequently, if the preheated inhomogeneous densified colloidal monolayer was subsequently oxygen reactive ion etched, the morphology of the monolayer evolved into different ordered arrays with rectangular-shaped PS particles because of the anisotropic property of RIE. When the preheated sample was etched for 600 s, the shape of PS particles was changed to rectangular particles with four necks linked with four of its neighboring particles. As a result, the morphology of the monolayer was converted to network-like arrays with rectangular-shaped PS particles (Fig. 3b). When the etching time was increased to 900 s, the size of the rectangular-shaped PS particles was decreased and the necks were broken. Therefore, the morphology of the monolayer was changed to PS arrays consisting of separated rectangular-shaped particles (Fig. 3c). All of these rectangular-shaped PS particle arrays, exhibiting a hexagonal arrangement like that of the pristine monolayer, are new colloidal lithographic nanopatterns firstly reported here.

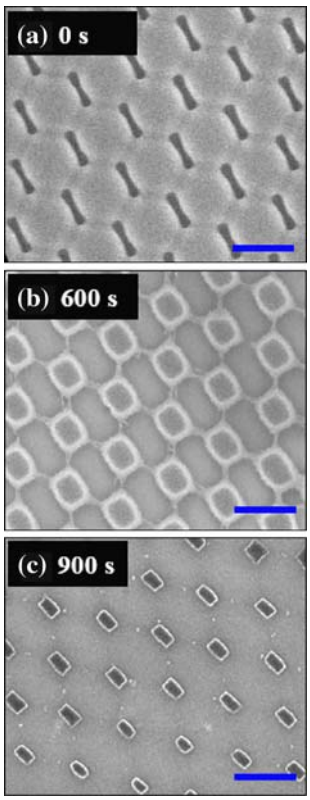

Fig. 3 SEM images of preheated inhomogeneous densified monolayer of PS spheres with 465 nm in diameter after oxygen RIE for different time: **a** 0 s, **b** 600 s, **c** 900 s, respectively. The *scale bar* is 500 nm in each image

Figure 4 shows another new type of colloidal nanopatterns: hexagonal-shaped PS particle arrays fabricated by preheating and oxygen RIE of self-assembled monolayer of 1,000 nm PS spheres. After exposure to the same oxygen RIE conditions for 30 min, the morphology of the preheated monolayer with face contact between neighboring spheres (Fig. 4b1) was converted to hexagonal-shaped PS particle arrays arranged hexagonally with long-range order (Fig. 4b2), which is very different from disordered elliptical-shaped PS particle pattern (Fig. 4a2) obtained from the nonpreheated sample with point contact between neighboring spheres (Fig. 4a1). Therefore, preheating, which deforms the contact between neighboring PS particles from point contact to face contact, is critical in the formation of this new colloidal nanopatterns of hexagonal-shaped PS particle arrays.

Our method can be extended to a double-layer of PS spheres to change the colloidal nanopatterns, as shown in Fig. 5. Different morphologies of colloid crystals were

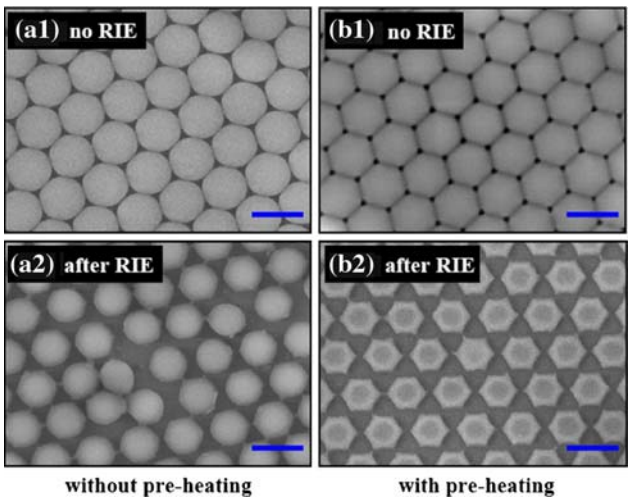

Fig. 4 SEM images of monolayer of PS spheres (1,000 nm in diameter): **a1**,**b1** before and after preheating; **a2**,**b2** after the same oxygen RIE conditions for the nonpreheated sample and preheated sample, respectively. The *scale bar* is 1,000 nm in each image

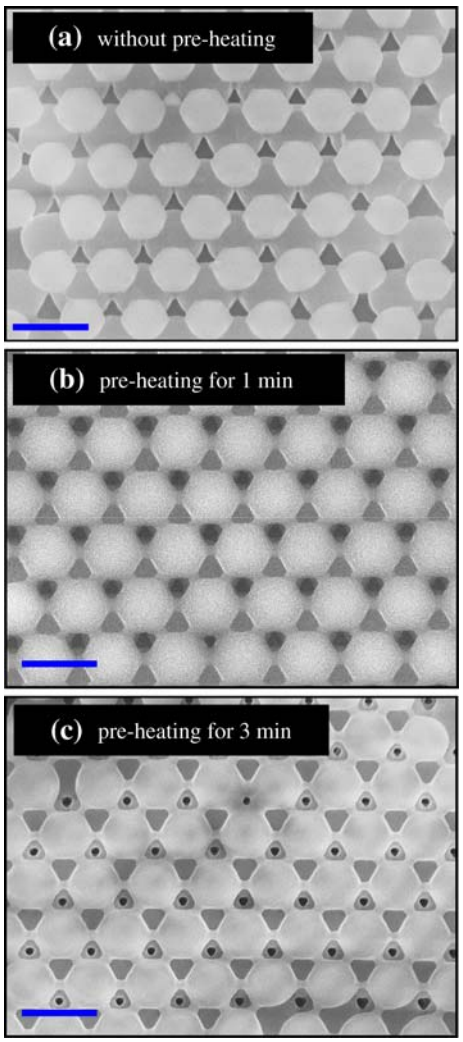

Fig. 5 SEM images of double-layer of PS spheres (1,000 nm in diameter) after the same oxygen RIE conditions with different preheating time: **a** 0 min, **b** 1 min, **c** 3 min, respectively. The *scale bar* is 1,000 nm in each image

produced by oxygen RIE of the double-layer of PS spheres (1,000 nm in diameter) preheated for different durations of 0, 1, and 3 min. Compared with the resulting shape of colloidal monolayer without preheating (Fig. 5a), the shape of the apertures changed gradually from triangle to round, and the size of the apertures became smaller and smaller by increasing the preheating time (Fig. 5b, c). These scale-down nanohole arrays are good masks for fabrication of nanodot arrays of other materials.

Conclusions

In summary, we have fabricated controllable PS particle structures with a long-range order by combination of preheating and oxygen RIE techniques. The neck length and neck width of the network pattern fabricated by oxygen RIE of preheated monolayer of PS spheres can be easily tuned from about 30 to 80 nm and 150 to 80 nm, respectively, by increasing the oxygen RIE time. Moreover, the hexagonal-shaped and rectangular-shaped PS particles and round nanoholes were obtained after oxygen RIE of monolayer and double layer of PS spheres with preheating, which differs noticeably from the elliptical-shaped PS particles and triangular nanoholes produced without preheating. The network pattern with controllable neck width and length and the hexagonal-shaped as well as rectangular-shaped PS particle arrays obtained with preheating are new colloidal lithographic nanopatterns, which raised hopes for NSL. Preheating plays a crucial role in fabricating these new long-range ordered PS particle arrays. These new colloidal nanopatterns have important applications in fields of catalysts, biosensors, and biomedical devices, especially in next-generation integrated nanophotonic devices, bimolecular labeling and identification [23].

References

1. J. Storhoff, R. Elghanian, R.C. Micuc, C.A. Mirkin, R.L. Letsinger, J. Am. Chem. Soc. **120**, 1959 (1998)
2. C. Hagleitner, A. Hierlemann, D. Lange, A. Kummer, N. Kerness, O. Brand, H. Baltes, Nature **414**, 293 (2001)
3. Y. Cui, Q.Q. Wei, H.K. Park, C.M. Leiber, Science **293**, 1289 (2001)
4. Y. Xia, E. Kim, X.M. Zhao, J.A. Rogers, M. Prentiss, G.M. Whitesides, Science **273**, 347 (1996)
5. Z. Liu, Z. Xie, X. Zhao, Z.Z. Gu, J. Mater. Chem. **18**, 3309 (2008)
6. Z.Z. Gu, H. Uetsuka, K. Takahashi, R. Nakajima, H. Onishi, A. Fujishima, O. Sato, Angew. Chem. Int. Ed. **42**, 894 (2003)
7. J.R. Jeong, S. Kim, S.H. Kim, J.A.C. Bland, S.C. Shin, S.M. Yang, Small **3**, 1529 (2007)
8. J. Aizpurua, P. Hanarp, D.S. Sutherland, M. Käll, G.W. Bryant, F.J.G. de Abajo, Phys. Rev. Lett. **90**, 057401 (2003)
9. J. Rybczynski, U. Ebels, M. Giersig, Colloids Surf. A Physicochem. Eng. Asp. **219**, 1 (2003)
10. Y. Xia, B. Gates, Y. Yin, Y. Lu, Adv. Mater. **12**, 693 (2000)
11. P. Jiang, T. Prasad, M.J. McFarland, V.L. Colvin, Appl. Phys. Lett. **89**, 011908 (2006)
12. M. Trau, D.A. Saville, I.A. Aksay, Science **272**, 706 (1996)
13. S.O. Lumsdon, E.W. Kaler, J.P. Williams, O.D. Velev, Appl. Phys. Lett. **82**, 949 (2003)
14. S. Reculusa, S. Ravaine, Chem. Mater. **15**, 598 (2003)
15. J. Rybczynski, U. Ebels, M. Giersig, Colloids Surf. A **219**, 1 (2003)
16. M.C. Gwinner, E. Koroknay, L. Fu, P. Patoka, W. Kandulski, M. Giersig, H. Giessen, Small **5**, 400 (2009)
17. D.G. Choi, H.K. Yu, S.G. Jang, S.M. Yang, J. Am. Chem. Soc. **126**, 7019 (2004)
18. B.J.Y. Tan, C.H. Sow, K.Y. Lim, F.C. Cheong, G.L. Chong, A.T.S. Wee, C.K. Ong, J. Phys. Chem. B **108**, 18575 (2004)
19. L. Yan, K. Wang, J. Wu, L. Ye, J. Phys. Chem. B **110**, 11241 (2006)
20. P. Wu, L. Peng, X. Tuo, X. Wang, J. Yuan, Nanotechnology **16**, 1693 (2005)
21. H. Li, J. Low, K.S. Brown, N. Wu, IEEE Sens. J. **8**, 880 (2008)
22. A. Kosiored, W. Kandulski, H. Glaczynska, M. Giersig, Small **1**, 439 (2005)
23. F.Q. Sun, W.P. Cai, Y. Li, B.Q. Cao, Y. Lei, L.D. Zhang, Adv. Funct. Mater. **14**, 283 (2004)